A Hydrothermal Investigation of the $^1/_2V_2O_5-H_2C_2O_4/H_3PO_4/NH_4OH$ System: Synthesis and Structures of $(NH_4)VOPO_4\cdot1.5H_2O$, $(NH_4)_{0.5}VOPO_4\cdot1.5H_2O$, $(NH_4)_2[VO(H_2O)_3]_2[VO(H_2O)][VO(PO_4)_2]_2\cdot3H_2O$, and $(NH_4)_2[VO(HPO_4)]_2(C_2O_4)\cdot5H_2O$

Junghwan Do, Ranko P. Bontchev, and Allan J. Jacobson*

Department of Chemistry, University of Houston, Houston, Texas 77204-5641

Received January 6, 2000

The $^1/_2V_2O_5-H_2C_2O_4/H_3PO_4/NH_4OH$ system was investigated using hydrothermal techniques. Four new phases, $(NH_4)VOPO_4\cdot1.5H_2O$ (**1**), $(NH_4)_{0.5}VOPO_4\cdot1.5H_2O$ (**2**), $(NH_4)_2[VO(H_2O)_3]_2[VO(H_2O)][VO(PO_4)_2]_2\cdot3H_2O$ (**3**), and $(NH_4)_2[VO(HPO_4)]_2(C_2O_4)\cdot H_2O$ (**4**), have been prepared and structurally characterized. Compounds **1** and **2** have layered structures closely related to $VOPO_4\cdot2H_2O$ and $A_{0.5}VOPO_4\cdot yH_2O$ (A = mono- or divalent metals), whereas **3** has a 3D open-framework structure. Compound **4** has a layered structure and contains both oxalate and phosphate anions coordinated to vanadium cations. Crystal data: $(NH_4)VOPO_4\cdot1.5H_2O$, tetragonal (*I*), space group *I*4/*mmm* (No. 139), $a = 6.3160(5)$ Å, $c = 13.540(2)$ Å, $Z = 4$; $(NH_4)_{0.5}VOPO_4\cdot1.5H_2O$, monoclinic, space group $P2_1/m$ (No. 11), $a = 6.9669(6)$ Å, $b = 17.663(2)$ Å, $c = 8.9304(8)$ Å, $\beta = 105.347(1)°$, $Z = 8$; $(NH_4)_2[VO(H_2O)_3]_2[VO(H_2O)][VO(PO_4)_2]_2\cdot3H_2O$, triclinic, space group $P\bar{1}$ (No. 2), $a = 10.2523(9)$ Å, $b = 12.263(1)$ Å, $c = 12.362(1)$ Å, $\alpha = 69.041(2)°$, $\beta = 65.653(2)°$, $\gamma = 87.789(2)°$, $Z = 2$; $(NH_4)_2[VO(HPO_4)]_2(C_2O_4)\cdot5H_2O$, monoclinic (*C*), space group *C*2/*m* (No. 12), $a = 17.735(2)$ Å, $b = 6.4180(6)$ Å, $c = 22.839(2)$ Å, $\beta = 102.017(2)°$, $Z = 6$.

Introduction

Vanadium phosphates and organophosphonates are a large class of compounds that has been studied in detail.[1−3] Specific compounds find application in oxidation catalysis,[4,5] and others have potential uses as solid sorbents and ion exchangers. The layered compound $VOPO_4\cdot2H_2O$ is one of the best known examples, and many compounds have been synthesized with closely related structures. For example, the mixed-valence A_x-$VOPO_4\cdot yH_2O$[6,7] phases were synthesized by redox intercalation reactions of $VOPO_4\cdot2H_2O$. Several other layered mixed-valence vanadium phosphate hydrates $A_{0.5}VOPO_4\cdot xH_2O$ (A = Na, $x = 2$; A = K, $x = 1.5$)[8] and divalent metal incorporated compounds $A_{0.5}VOPO_4\cdot2H_2O$ (A = Ca, Ba, Sr, Co, Ni, Cu, Pb)[9−13] were subsequently prepared hydrothermally.

In a recent paper, the effect of conditions on the synthesis of vanadium(IV) phosphate phases from solution was described. Oxalic acid was used as the reducing agent to prepare a V(IV) solution from V(V) starting materials.[14] From this solution a series of V(IV) phosphate hydrates were isolated by varying crystallization conditions. Oxalate anions may also directly coordinate transition metals, and several transition metal (Mn, In, Ga, Al, and Fe) systems have been synthesized in which the transition metal cations are coordinated by both phosphate and oxalate anions.[15−22] Most recently an example of a V(IV) linear chain oxalato−phosphate, $(C_4H_{12}N_2)[VO(C_2O_4)HPO_4]$,[23] was reported. The structure of this compound is related to that of $VOHPO_4\cdot4H_2O$.[24] These oxalato−phosphates are limited in number but show several modes of oxalate binding and different framework connectivities.

In this paper, we report the results of a systematic study of reactions of V_2O_5 in the $H_2C_2O_4/H_3PO_4/NH_4OH$ system using hydrothermal syntheses. The oxalic acid in the syntheses plays

* Author to whom correspondence should be addressed. Tel: (713) 743-2785. Fax: (713) 743-2787. E-mail: ajjacob@uh.edu.

(1) Amorós, P.; Dolores Marcos, M.; Beltrán-Porter, A.; Beltrán-Porter, D. *Curr. Opin. Solid State Mater. Sci.* **1999**, *4*, 123.
(2) Zubieta, J. *Comments Inorg. Chem.* **1994**, *16*, 153.
(3) Kalousova, J.; Votinsky, J.; Benes, L.; Melanova, K.; Zima, V. *Collect. Czech. Chem. Commun.* **1998**, *63*, 1.
(4) Gai, P. L.; Kourtakis, K. *Science* **1995**, *267*, 661.
(5) Coulston, G. W.; Bare, S. R.; Kung, H.; Birkeland, K.; Bethke, G. K.; Harlow, R.; Herron, N.; Lee, P. L. *Science* **1997**, *275*, 191.
(6) Johnson, J. W.; Jacobson, A. J. *Angew. Chem., Int. Ed. Engl.* **1983**, *22*, 412.
(7) Jacobson, A. J.; Johnson, J. W.; Brody, J. F.; Scanlon, J. C.; Lewandowski, J. T. *Inorg. Chem.* **1985**, *24*, 1782.
(8) Wang, S.-L.; Kang, H.-Y.; Cheng, C.-Y.; Lii, K.-H. *Inorg. Chem.* **1991**, *30*, 3496.
(9) Kang, H.-Y.; Lee, W.-C.; Wang, S.-L.; Lii, K.-H. *Inorg. Chem.* **1992**, *31*, 4743.
(10) Roca, M.; Marcos, M. D.; Amoros, P.; Alamo, J.; Beltrán-Porter, A.; Beltrán-Porter, D. *Inorg. Chem.* **1997**, *36*, 3414.
(11) Lii, K.-H.; Wu, L.-S.; Gau, H.-M. *Inorg. Chem.* **1993**, *32*, 4153.
(12) Haushalter, R. C.; Soghomonian, V.; Chen, Q.; Zubieta, J. *J. Solid State Chem.* **1993**, *105*, 512.
(13) Zhang, Y.; Clearfield, A.; Haushalter, R. C. *J. Solid State Chem.* **1995**, *117*, 157.
(14) Fratzky, D.; Gotze, Th.; Worzala, H.; Meisel, M. *Mater. Res. Bull.* **1998**, *33*, 635.
(15) Averbuch-Pouchot, M. T.; Durif, A. *Acta Crystallogr.* **1990**, *C46*, 965.
(16) Huang, Y.-F.; Lii, K.-H. *J. Chem. Soc., Dalton Trans.* **1998**, 4085.
(17) Lightfoot, P.; Lethbridge, Z. A. D.; Morris, R. E.; Wragg, D. S.; Wright, P. A.; Kvick, Å.; Vaughan, G. B. M. *J. Solid State Chem.* **1999**, *143*, 74.
(18) Lethbridge, Z. A. D.; Lightfoot, P. *J. Solid State Chem.* **1999**, *143*, 53.
(19) Chen, C.-Y.; Chu, P. P.; Lii, K.-H. *Chem. Commun. (Cambridge)* **1999**, 1473.
(20) Lin, H.-M.; Lii, K.-H.; Jiang, Y.-C.; Wang, S.-L. *Chem. Mater.* **1999**, *11*, 499.
(21) Choudhury, A.; Natarajan, S.; Rao, C. N. R. *Chem. Mater.* **1999**, *11*, 2316.
(22) Choudhury, A.; Natarajan, S.; Rao, C. N. R. *J. Solid State Chem.* **1999**, *146*, 538.
(23) Tsai, Y.-M.; Wang, S.-L.; Huang, C.-H.; Lii, K.-H. *Inorg. Chem.* **1999**, *38*, 4183.
(24) Leonowicz, M. E.; Johnson, J. W.; Brody, J. F.; Shannon, H. F.; Newsam, J. W. *J. Solid State Chem.* **1985**, *56*, 370.

10.1021/ic0000303 CCC: $19.00
Published on Web 06/24/2000

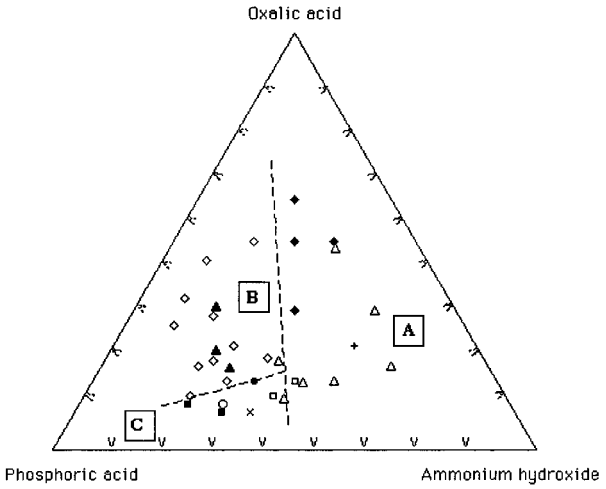

● $(NH_4)(VOPO_4)\cdot 1.5H_2O$ (**1**)	pH = 5.73
■ $(NH_4)_{0.5}(VOPO_4)\cdot 1.5H_2O$ (**2**)	$2.10 \le pH \le 3.72$
◇ $(NH_4)_3[(VO)_3(V_2O_2)(PO_4)_4(H_2O)_7]\cdot 2H_2O$ (**3**)	$1.87 \le pH \le 5.23$
▲ $(NH_4)_2[VO(HPO_4)]_2(C_2O_4)\cdot H_2O$ (**4**)	$3.29 \le pH \le 3.75$
□ $(NH_4)_2(VO)(VPO_7)$	$5.73 \le pH \le 5.88$
○ $(NH_4)VOPO_4$	pH = 3.72
△ gray/brown powder	$5.39 \le pH \le 7.33$
◆ blue/green gel/powder	$3.43 \le pH \le 6.85$
+ green solution	pH = 7.37
× yellow solution	pH = 5.90

Figure 1. Three-component mixture diagram for $H_2C_2O_4/H_3PO_4/NH_4OH$, showing the relationship between reaction mixing ratios and identities of the solid phases produced at 140 °C. The mole ratio V_2O_5/oxalic acid = 1/2.

the role of a reducing agent but in some regions of reactant composition also acts as a ligand. As a result of this study, reaction conditions for the synthesis of two layered vanadium phosphates, $(NH_4)VOPO_4\cdot 1.5H_2O$ (**1**) and $(NH_4)_{0.5}VOPO_4\cdot 1.5H_2O$ (**2**), with structures closely related to $VOPO_4\cdot 2H_2O$ were established. Compound **1** was previously obtained in microcrystalline form by electrochemical hydrothermal synthesis.[25] A new framework structure, $(NH_4)_2[VO(H_2O)_3]_2[VO(H_2O)][VO(PO_4)_2]_2\cdot 3H_2O$ (**3**), and a vanadium oxalato−phosphate, $(NH_4)_2[VO(HPO_4)]_2(C_2O_4)\cdot 5H_2O$ (**4**), were obtained in the same reaction system. Single crystals were obtained, and the structures of **1**−**4** were determined by X-ray diffraction.

Experimental Section

Synthesis. The $^1/_2V_2O_5-H_2C_2O_4/H_3PO_4/NH_4OH$ system was investigated as function of the initial compositions of the reactants in a systematic way. Hydrothermal reactions were carried out in 23-mL capacity Teflon-lined stainless steel Parr hydrothermal reaction vessels at 140 °C for 3 days. The solid products were recovered by vacuum filtration and washed with water. All the phases are stable in air and water. The phases present in a series of reactions with different initial reactant compositions are shown in Figure 1.

Green polyhedral crystals of $(NH_4)(VOPO_4)\cdot 1.5H_2O$ (**1**) were prepared from the reaction of 0.0909 g of V_2O_5 (0.5 mmol), 0.0900 g of $H_2C_2O_4$ (1 mmol), 0.21 mL of H_3PO_4 (3 mmol; 85 wt % solution in H_2O), 0.26 mL of NH_4OH (2 mmol; 29.6 wt % aqueous solution), and 3 mL of water. The initial solution pH was 2.28. Product recovery (87% yield based on V) gave $(NH_4)(VOPO_4)\cdot 1.5H_2O$ single crystals together with a small quantity of unidentified black material. The pH after the reaction was 5.73. $(NH_4)(VOPO_4)\cdot 1.5H_2O$ could not be synthesized by using a stoichiometric reaction with $V:P:NH_4 = 1:1:1$. An unidentified pale greenish gray microcrystalline phase was formed instead.

Dark green platy crystals of $(NH_4)_{0.5}(VOPO_4)\cdot 1.5H_2O$ (**2**) form over a narrow range of conditions (Figure 1). The product was accompanied by either **3** or red crystals of NH_4VOPO_4.[26] The best crystals of **2** were formed in 74% yield from the reaction of 0.0454 g of V_2O_5 (0.25 mmol), 0.0450 g of $H_2C_2O_4$ (0.5 mmol), 0.21 mL of H_3PO_4 (3 mmol; 85 wt % solution in H_2O), 0.13 mL of NH_4OH (1 mmol; 29.6 wt % aqueous solution), and 3 mL of water. The pH values before and after reaction were 1.93 and 2.10, respectively. In **2** the degree of vanadium reduction ($1V^V + 1V^{IV}$) is less than in **1** (all V(IV)).

$(NH_4)_2[VO(H_2O)_3]_2[VO(H_2O)][VO(PO_4)_2]_2\cdot 3H_2O$ (**3**) was obtained over a wide range of conditions (Figure 1). The best crystals of **3** were prepared from the reaction of 0.1364 g of V_2O_5 (0.75 mmol), 0.1350 g of $H_2C_2O_4$ (1.5 mmol), 0.21 mL of H_3PO_4 (3 mmol; 85 wt % solution in H_2O), 0.065 mL of NH_4OH (0.5 mmol; 29.6 wt % aqueous solution), and 3 mL of water. Blue platy crystals (31% yield based on V) were obtained as a single phase. The compound **3** is obtained in the pH range 1.87−5.23. Reactions at lower pH give higher yields, and a single-phase product is formed at very low pH 1.87.

The best crystals of $(NH_4)_2[VO(HPO_4)]_2(C_2O_4)\cdot 5H_2O$ (**4**) were synthesized as plates in 96% yield from the reaction of 0.0909 g of V_2O_5 (0.5 mmol), 0.0900 g of $H_2C_2O_4$ (1 mmol), 0.17 mL of H_3PO_4 (2.5 mmol; 85 wt % solution in H_2O), 0.13 mL of NH_4OH (1 mmol; 29.6 wt % aqueous solution), and 3 mL of water. The solution pH values before and after the reaction were 1.89 and 3.29, respectively. In all three of the reactions shown in Figure 1, **4** was always accompanied by **3** as a minority phase. Compound **4** is obtained only in the pH range 3.3−3.8.

Characterization. Infrared spectra were recorded on a Mattson FTIR 5000 spectrometer within the range 400−4000 cm^{-1} using the KBr pellet method. Thermogravimetric analyses were carried out in air at a heating rate of 2 °C/min, using a high-resolution TGA 2950 thermogravimetric analyzer (TA Instruments). Magnetic measurements were made with an Oxford Instruments vibrating sample magnetometer in the temperature range $4 < T$ (K) < 290 with an applied magnetic field of 1 T.

Crystal Structures. The crystal structures of **1**−**4** were determined by single-crystal X-ray diffraction methods. Preliminary examination and data collection were performed on a SMART platform diffractometer equipped with a 1K CCD area detector using graphite-monochromatized Mo Kα radiation at room temperature. A hemisphere of data (1271 frames at 5 cm detector distance) was collected using a narrow-frame method with scan widths of 0.30° in ω and an exposure time of 30 s/frame. The first 50 frames were remeasured at the end of data collection to monitor instrument and crystal stability, and the maximum correction applied on the intensities was <1%. The data were integrated using the Siemens SAINT program,[27] with the intensities corrected for the Lorentz factor, polarization, air absorption, and absorption due to variation in the path length through the detector faceplate. The program SADABS was used for the absorption correction.[28] Additional crystallographic details for **1**−**4** are given in Table 1. In all cases satisfactory refinements were obtained with the highest symmetry centrosymmetric space groups consistent with the systematic absence conditions.

The initial positions for all atoms were obtained using direct methods, and the structures were refined by full-matrix least-squares techniques with the use of the SHELXTL crystallographic software package.[29] The

(25) Liu, L.; Wang, X.; Bontchev, R.; Ross, K.; Jacobson, A. J. *J. Mater. Chem.* **1999**, *9*, 1585−1589.

(26) Haushalter, R. C.; Chen, Q.; Soghomonian, V.; Zubieta, J.; O'Connor, C. J. *J. Solid State Chem.* **1994**, *108*, 128.

(27) *SAINT*, Version 4.05; Siemens Analytical X-ray Instruments: Madison, WI, 1995.

(28) Sheldrick, G. M. *Program SADABS*; University of Gottingen: Gottingen, Germany, 1995.

Table 1. Crystallographic Details of **1**−**4**

	1	**2**	**3**	**4**
empirical formula	$H_7NO_{6.5}PV$	$H_5N_{0.5}O_{6.5}PV$	$H_{28}N_2O_{31}P_4V_5$	$C_2H_{12}N_2O_{15}P_2V_2$
fw	206.97	197.96	930.82	503.98
space group	*I*4/*mmm* (No. 139)	$P2_1/m$ (No. 11)	$P\bar{1}$ (No. 2)	*C*2/*m* (No. 12)
a, Å	6.3160(5)	6.9669(6)	10.2523(9)	17.735(2)
b, Å	6.3160(5)	17.663(2)	12.263(1)	22.839(2)
α, deg	90	90	69.041(2)	90
β, deg	90	105.347(1)	65.653(2)	102.017(2)
γ, deg	90	90	87.789(2)	90
V, Å^3	540.14(9)	1059.7(2)	1311.3(2)	2542.7(4)
Z	4	8	2	6
T, K	293(2)	293(2)	293(2)	293(2)
λ, Å	0.71073	0.71073	0.71073	0.71073
ρ, calcd g/cm^3	2.034	2.481	2.271	1.975
μ, cm^{-1}	20.57	21.41	20.82	13.79
crystal size, mm^3	0.28 × 0.17 × 0.13	0.32 × 0.30 × 0.06	0.22 × 0.19 × 0.02	0.24 × 0.21 × 0.05
R ($I > 2\sigma(I)$)	0.0323	0.0582	0.0715	0.0577
R_w[a]	0.0887	0.1360	0.1767	0.1383
A, *B*[a]	0.05, 1.98	0.00, 17.79	0.0283, 23.16	0.0319, 20.41

[a] $R_w = [\Sigma w(|F_o| - |F_c|)^2/\Sigma w|F_o|^2]^{1/2}$; $w = 1/[\sigma^2(F_o^2) + (AP)^2 + BP]$; $P = [\mathrm{Max}(F_o^2,0) + 2F_c^2]/3$ (all data).

R values for the final cycle of the refinements based on F_o^2 are given in Table 1. In all phases, no unusual trends were found in the goodness of fit as a function of F_o^2, sin θ/λ, and Miller indices. Final values of selected bond lengths are given in Table 2.

Results and Discussion

Synthesis. The $^1/_2V_2O_5$−$H_2C_2O_4$/H_3PO_4/NH_4OH system was studied as a function of the initial compositions. The reactions shown in the mixture diagram (Figure 1) result in the formation of six distinct compounds. Single crystals of three new hydrated ammonium vanadium phosphates, one ammonium vanadium oxalato−phosphate, and two known phases $(NH_4)VOPO_4$[26] and $(NH_4)_2(VO)(V_{1-x}P_{1+x}O_7)$[30,31] were synthesized. The compound $NH_4VOPO_4 \cdot H_2O$,[32] which has a structure related to that of $VO(HPO_4) \cdot 4H_2O$, was not observed under the conditions shown in Figure 1. The figure is divided into three regions, A, B, and C, that qualitatively represent composition regions where different compound types are formed.

All of the compounds that were identified and isolated as single crystals were prepared in the H_3PO_4-rich region of the mixture diagram (regions B and C). Only poorly crystalline phases or gels were formed in the $H_2C_2O_4$- and NH_4OH-rich regions ($3.4 \leq pH \leq 7.3$) (region A). These phases could not be identified, but infrared measurements indicated that they did not contain oxalate anions.

In region B, the predominant phase observed is **3.** This compound forms over a wide range of reactant compositions with $1.8 \leq pH \leq 5.2$ and contains only V(IV). Compound **4**, the only phase synthesized that contains oxalate anions, was also isolated in region B. **4** is formed together with **3** in a narrow range of composition and only in a very narrow pH range ($3.3 \leq pH \leq 3.8$).

Four compounds were formed in region C: $NH_4VOPO_4 \cdot 1.5H_2O$ (**1**); $(NH_4)_{0.5}(VOPO_4) \cdot 1.5H_2O$ (**2**); and two known phases, NH_4VOPO_4[26] and $(NH_4)_2(VO)(V_{1-x}P_{1+x}O_7)$.[30,31] Phase **1** and NH_4VOPO_4 contain V(IV) only whereas **2** and $(NH_4)_2(VO)(V_{1-x}P_{1+x}O_7)$ are mixed-valence (IV and V) compounds. Lowering the oxalate concentration in the solution favors the formation of V(V)-containing phases and gives rise to the boundary between regions B and C.

Characterization. The IR spectra of **1**−**4** are shown in Figure 2. Vibration modes for P−O, V−O, and V═O are observed at 1121, 1005, 679, 540, 438 cm^{-1}, **1**; 1150, 1063, 1021, 959, 895, 681, 569, 531 cm^{-1}, **2**; 1099, 1049, 1029, 982, 887, 615, 561 cm^{-1}, **3**; 1117, 1076, 993, 812, 648, 525, 486 cm^{-1}, **4**. Strong absorption bands for N−H and O−H bending and stretching vibrations are observed at 3364, 3061, 1641, 1491, 1431 cm^{-1}, **1**; 3530, 3144, 1624, 1417, 1433 cm^{-1}, **2**; 3502, 3144, 1630, 1409, 1437 cm^{-1}, **3**; 3445, 3148, 1402 cm^{-1}, **4**. Additional bands due to C−O vibrations for **4** occur at 1674, 1356, 1316, 902 cm^{-1}.

Thermogravimetric analysis of **2** shows that the evolution of NH_3 and water molecules occurs from room temperature to ∼470 °C, and that the oxidation of V^{4+} to V^{5+} is complete at ∼770 °C. Assuming that the residue corresponds to $^1/_2V_2O_5$ and $^1/_2P_2O_5$, then the observed weight loss (18.32%) is in good agreement with the calculated value (18.20%) for the composition $(NH_4)_{0.5}[VOPO_4] \cdot 1.5H_2O$. For **3** the evolution of NH_3 and water molecules from the structure also is observed to occur below ∼470 °C in several steps. Assuming that the glassy residue corresponds to $^5/_2V_2O_5$ and $2P_2O_5$, the overall observed weight loss (20.80%) is in good agreement with the value calculated for the composition $(NH_4)_2[VO(H_2O)_3]_2[VO(H_2O)][VO(PO_4)_2]_2 \cdot 3H_2O$ (20.65%). For **4** the evolution of crystal water occurs below 200 °C, and evolution of NH_3 and H_2O and carbon oxides was observed between ∼200 °C and 350 °C (weight loss, calcd 23.45%, exptl 23.96%). The evolution of water molecules from the structure and the oxidation of V^{4+} to V^{5+} is complete near 770 °C. Thermogravimetric analysis data were previously reported for **1** and gave a composition $NH_4VOPO_4 \cdot 1.4H_2O$.[25]

Magnetic susceptibility data for **2** revealed paramagnetic behavior over the temperature range 4.5−250 K. The data were modeled by the Curie−Weiss function $\chi_m = \chi_0 + C_m/(T - \theta)$, $\chi_0 = -2.09 \times 10^{-4}$ emu/mol, $C_m = 0.3812$ emu K/mol, and $\theta = -6.5$ K. The calculated effective magnetic moment $\mu_{eff} = 1.75\ \mu_B$ is in good agreement with the expected value of 1.73 μ_B, assuming that one-half of the vanadium atoms in the formulas $(NH_4)[VOPO_4]_2 \cdot 3H_2O$ are present as V(IV). Magnetic susceptibility data for **3** also revealed paramagnetic behavior over the temperature range 4.0−288 K. The data were fitted by the Curie equation: $\chi_m = \chi_0 + C_m/T$, $\chi_0 = -4.45 \times 10^{-4}$

(29) Sheldrick, G. M. *SHELXTL*, Version 5.03; Siemens Analytical X-ray Instruments: Madison, WI, 1995.
(30) Ninclaus, C.; Retoux, R.; Riou, D.; Férey, G. *J. Solid State Chem.* **1996**, *122*, 139.
(31) Boudin, S.; Grandin, A.; Labbe, P.; Raveau, B. *Acta Crystallogr.* **1996**, *C52*, 2668.
(32) Bircsk, Z.; Harrison, W. T. A. *Inorg. Chem.* **1998**, *37*, 5387.

Table 2. Selected Bond Lengths (Å) for **1**−**4**

			Compound **1**[a]				
V−O(1)	1.578(5)	V−O(2) #1	2.000(2)	P−O(2) #4	1.544(2)	P−O(2) #5	1.544(2)
V−O(2) #2	2.000(2)	V−O(2) #3	2.000(2)	P−O(2)	1.544(2)	P−O(2) #6	1.544(2)
V−O(2)	2.000(2)						
			Compound **2**[a]				
V(1)−O(12)	1.604(9)	V(1)−O(2)	2.024(5)	V(3)−O(7)	1.948(6)	V(3)−O(6)	1.971(6)
V(1)−O(2) #1	2.024(5)	V(1)−O(1)	2.033(5)	V(3)−O(9)	1.972(6)	V(3)−O(10)	2.376(11)
V(1)−O(1) #1	2.033(5)	V(1)−O(11)	2.30(1)	P(1)−O(7)	1.520(6)	P(1)−O(2) #2	1.524(6)
V(2)−O(13)	1.568(9)	V(2)−O(3)	1.877(5)	P(1)−O(5) #3	1.547(6)	P(1)−O(9) #3	1.549(6)
V(2)−O(3) #1	1.877(5)	V(2)−O(5) #1	1.913(6)	P(2)−O(1)	1.520(6)	P(2)−O(8) #2	1.528(6)
V(2)−O(5)	1.913(6)	V(2)−O(4)	2.302(9)	P(2)−O(3)	1.550(6)	P(2)−O(6)	1.553(6)
V(3)−O(14)	1.580(6)	V(3)−O(8)	1.948(6)				
			Compound **3**[a]				
V(1)−O(25)	1.599(6)	V(1)−O(12)	1.970(6)	V(5)−O(23)− #4	2.235(6)	V(5)−V(6B)	3.045(4)
V(1)−O(3)	1.972(6)	V(1)−O(21)	1.980(6)	V(6A)−V(6B)	0.604(3)	V(6A)−O(24)	1.666(6)
V(1)−O(6)	2.011(6)	V(1)−O(27)	2.389(7)	V(6A)−O(9) #6	1.956(7)	V(6A)−O(19) #6	1.982(6)
V(2)−O(10)	1.589(6)	V(2)−O(4)	1.998(6)	V(6A)−O(8) #2	2.015(6)	V(6A)−O(2) #2	2.012(7)
V(2)−O(28)	2.010(6)	V(2)−O(18)	2.051(7)	V(6A)−O(23)	2.247(6)	V(6A)−V(4) #1	3.085(4)
V(2)−O(13)	2.052(6)	V(2)−O(17)	2.288(6)	V(6B)−O(23)	1.647(6)	V(6B)−O(8) #2	1.948(6)
V(3)−O(26)	1.576(6)	V(3)−O(1)	1.994(6)	V(6B)−O(2) #2	1.965(7)	V(6B)−O(9) #6	2.002(7)
V(3)−O(11)	1.997(6)	V(3)−O(7)	2.033(6)	V(6B)−O(19) #6	2.057(6)	V(6B)−O(24)	2.262(6)
V(3)−O(14)	2.063(6)	V(3)−O(5)	2.322(6)	P(1)−O(6)	1.526(6)	P(1)−O(19)	1.529(5)
V(4)−V(4) #1	0.586(5)	V(4)−O(24) #1	1.654(6)	P(1)−O(4)	1.546(6)	P(1)−O(15)	1.549(5)
V(4)−O(16) #2	1.975(7)	V(4)−O(20) #2	1.979(7)	P(2)−O(3)	1.502(6)	P(2)−O(22)	1.534(5)
V(4)−O(16) #3	2.018(7)	V(4)−O(20) #3	2.039(7)	P(2)−O(9)	1.549(6)	P(2)−O(1)	1.545(6)
V(4)−O(24)	2.235(6)	V(4)−V(6A) #1	3.085(4)	P(3)−O(16)	1.521(6)	P(3)−O(12) #2	1.522(6)
V(5)−V(5) #4	0.596(5)	V(5)−O(23)	1.641(6)	P(3)−O(28)	1.547(6)	P(3)−O(2)	1.554(6)
V(5)−O(22) #5	1.959(7)	V(5)−O(22) #6	1.979(7)	P(4)−O(8)	1.533(5)	P(4)−O(20)	1.540(6)
V(5)−O(15) #6	2.011(7)	V(5)−O(15) #5	2.004(7)	P(4)−O(21) #2	1.538(6)	P(4)−O(11) #7	1.556(6)
			Compound **4**[a]				
V(1)−O(8)	1.609(7)	V(1)−O(4)	1.984(7)	V(2)−O(5)	2.074(8)	V(2)−O(2)	2.284(8)
V(1)−O(7)	2.007(5)	V(1)−O(7) #1	2.007(5)	V(3)−O(17)	1.576(8)	V(3)−O(14)	1.994(8)
V(1)−O(6)	2.091(6)	V(1)−O(1)	2.297(7)	V(3)−O(16)	1.999(5)	V(3)−O(16) #1	1.999(5)
V(2)−O(10)	1.584(8)	V(2)−O(3)	1.973(7)	V(3)−O(15)	2.066(7)	V(3)−O(13)	2.321(7)
V(2)−O(9)	2.017(5)	V(2)−O(9) #2	2.017(5)				
P(1)−O(16) #3	1.527(5)	P(1)−O(16) #4	1.527(5)	P(2)−O(7) #2	1.526(5)	P(2)−O(11)	1.578(8)
P(1)−O(14)	1.543(8)	P(1)−O(18)	1.594(7)	P(3)−O(9) #2	1.507(5)	P(3)−O(9) #5	1.507(5)
P(2)−O(3)	1.509(7)	P(2)−O(7)	1.526(5)	P(3)−O(4)	1.535(7)	P(3)−O(12)	1.597(9)
O(1)−C(2)	1.230(11)	O(2)−C(1)	1.218(12)	C(1)−O(6) #6	1.263(11)	C(1)−C(2) #6	1.487(13)
O(5)−C(2) #6	1.310(12)	O(6)−C(1) #7	1.263(11)	C(2)−O(5) #7	1.310(12)	C(2)−C(1) #7	1.487(13)
O(13)−C(3)	1.272(11)	O(15)−C(3) #8	1.204(12)	C(3)−O(15) #8	1.204(12)	C(3)−C(3) #8	1.64(2)

[a] Symmetry transformations used to generate equivalent atoms for **1**: #1 $-y, x, z$; #2 $y, -x, z$; #3 $-x, -y, z$; #4 $-x+1, -y, z$; #5 $-y+{}^1/_2, x-{}^1/_2, -z+{}^1/_2$; #6 $y+{}^1/_2, -x+{}^1/_2, -z+{}^1/_2$. For **2**: #1 $x, -y+{}^3/_2, z$; #2 $-x+1, -y+1, -z+2$; #3 $-x+1, -y+1, -z+3$. For **3**: #1 $-x+1, -y+1, -z$; #2 $x, y, z-1$; #3 $-x+1, -y+1, -z+1$; #4 $-x, -y, -z+1$; #5 $-x+1, -y, -z+1$; #6 $x-1, y, z$. For **4**: #1 $x, -y, z$; #2 $x, -y-1, z$; #3 $-x+{}^1/_2, -y+{}^1/_2, -z$; #4 $-x+{}^1/_2, y-{}^1/_2, -z$; #5 $x, y+1, z$; #6 $x-{}^1/_2, y-{}^1/_2, z$; #7 $x+{}^1/_2, y+{}^1/_2, z$. #8 $-x, -y, -z$.

emu/mol, and $C_m = 1.869$ emu K/mol. The calculated effective magnetic moment $\mu_{eff} = 3.867\ \mu_B$ is in agreement with the expected value of 3.87 μ_B, assuming that all five vanadium atoms in the $(NH_4)_2[VO(H_2O)_3]_2[VO(H_2O)][VO(PO_4)_2]_2 \cdot 3H_2O$ are present as V(IV). The magnetic measurements for **4** also indicated a V^{4+} oxidation state with $\chi_0 = -7.0 \times 10^{-5}$ emu/mol, $C_m = 0.3692$ emu K/mol, $\theta = -4.5$ K, and $\mu_{eff} = 1.72\ \mu_B$.

Crystal Structures. The structure of **1** consists of $VOPO_4$ layers of VO_5 square pyramids and PO_4 tetrahedra with NH_4^+ cations and water molecules between the layers (Figures 3 and 4). One crystallographically unique V atom has a short vanadium oxygen (vanadyl) bond V═O (1.578(5) Å) and four equivalent equatorial V−O bonds (2.000(2) Å). The four equatorial oxygen atoms are shared with four phosphate tetrahedra, and each tetrahedron is connected to four distorted octahedra to make up the layers. The NH_4^+ cations and water molecules occupy sites between the layers. They are indistinguishable because they are disordered over the one crystallographically distinct atom site between the layers. The BVS value calculated for V is 3.98, in good agreement with the expected value of 4.00 for V(IV).[33]

The structure of **2** consists of $VOPO_4 \cdot H_2O$ layers of VO_6 distorted octahedra and PO_4 tetrahedra and interlayer NH_4^+ cations and water molecules (Figures 5 and 6). The four equatorial oxygen atoms in each VO_6 octahedron are shared with four PO_4 tetrahedra. One of the axial V−O bonds in each octahedron is a vanadyl group V═O (1.61(1) Å, V(1); 1.57(1) Å, V(2); 1.582(6) Å, V(3)). The long V−O bonds (2.32(1) Å, V(1); 2.310(9) Å, V(2); 2.372(7) Å, V(3)) to coordinated water molecules are trans to the short V═O bonds. The BVS calculation gives values of 3.92, 5.26, and 4.54 for V(1), V(2), and V(3), respectively, indicating oxidation states of 4.00 for V(1), 5.00 for V(2), and an average of 4.5 for V(3). One interlayer site is fully occupied and assigned to the NH_4^+ cation. The NH_4^+ cation H-bonds with seven neighboring oxygen atoms in the layers (Figure 7). The water molecules between the layers are disordered.

(33) Brese, N. E.; O'Keeffe, M. *Acta Crystallogr.* **1991**, *B47*, 192.

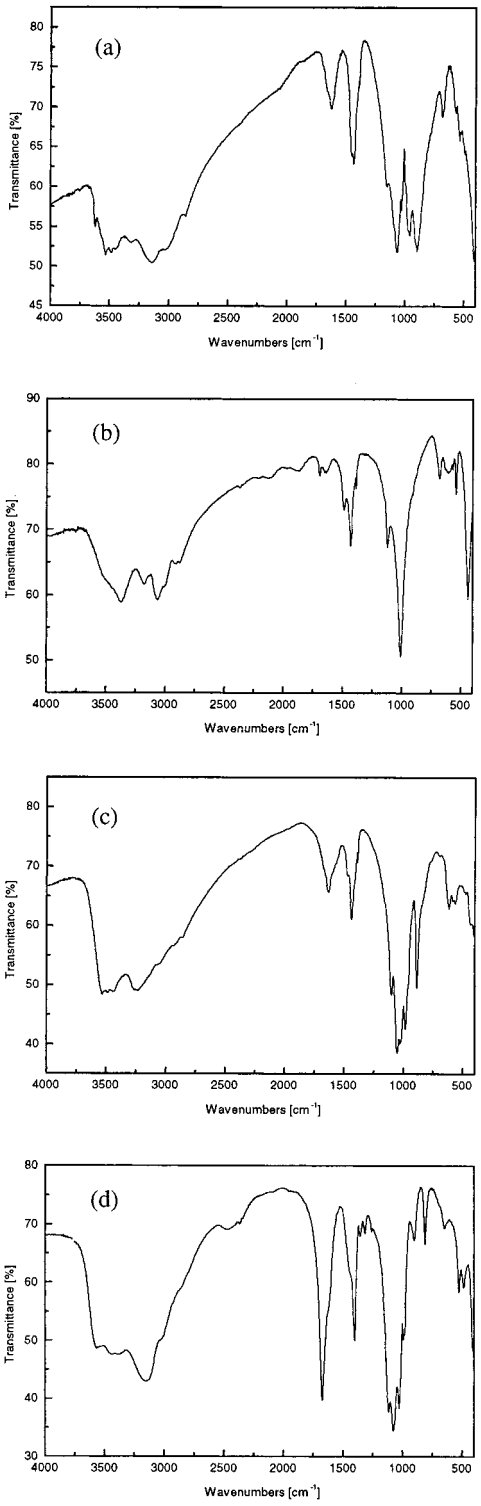

Figure 2. IR spectra of **1** (a), **2** (b), **3** (c), and **4** (d).

The structures of **1** and **2** are closely related to the tetragonal layer structure of $VOPO_4 \cdot 2H_2O$,[34] and other layered mixed-valence vanadium phosphate hydrates containing interlayer metal cations[6−13] and (piperazineH_2)$VOPO_4$.[35,36] The structures of **1** and **2** may be thought of as arising from the insertion of NH_4^+ into $VOPO_4 \cdot 2H_2O$ with full (**1**) or partial (**2**) reduction

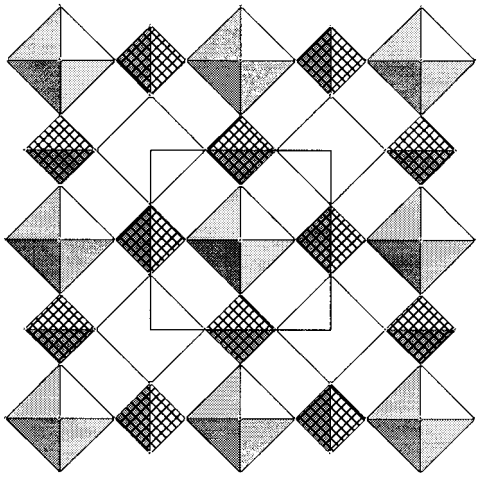

Figure 3. Polyhedral projection of the $VOPO_4$ layers in **1** viewed down the *c* axis. The VO_5 and PO_4 units are shown as square pyramids and hatched tetrahedra.

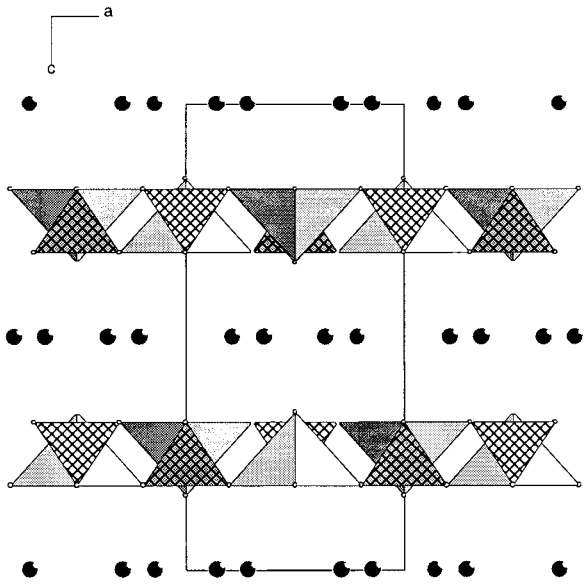

Figure 4. Projection of the structure of **1** in the [010] direction. The VO_5 and PO_4 units are shown as square pyramids and hatched tetrahedra.

of V^{5+} to V^{4+}. The modifications to the local coordination of V atoms and to the stacking arrangement of the vanadium phosphate layers relative to parent compound that occur are similar to those observed in compounds containing interlayer monovalent or divalent cations. The local geometry of V^{4+} in **1**, $NH_4VOPO_4 \cdot H_2O$,[32] (piperazineH_2)$VOPO_4$,[35,36] and $M(VOPO_4)_2 \cdot 4H_2O$ (M = Co, Ni)[9−13] is square pyramidal, whereas in **2**, $VOPO_4 \cdot 2H_2O$,[6,7] and $M_{0.5}VOPO_4 \cdot nH_2O$ (A = Ca, Sr, Ba, Cu, Pb, Na, K)[8−13] distorted octahedra are found.

In **2**, the presence of four inequivalent equatorial V−O bonds leads to puckered $VOPO_4 \cdot H_2O$ layers (Figure 6). The puckering isolates the interlayer solvent molecules into clusters surrounded by NH_4^+ cations. The arrangement is reminiscent of domains in staged intercalation compounds. The interlayer separations for **1** and **2** are 6.770 and 6.967 Å, respectively, which are shorter than that of $VOPO_4 \cdot 2H_2O$ (7.403 Å) and longer than those of K (6.38 Å), Na (6.53 Å), Ca(6.30 Å), Ba (6.39 Å), Sr (6.32 Å), Cu (6.42 Å), and Pb (6.34 Å) compounds.[9−13] The interlayer separation for **1** is similar to the values found for the Co (6.714 Å) and Ni (6.667 Å) compounds which have the same stacking arrangement as **1**. The average in plane dimensions

(34) Tietze, H. R. *Aust. J. Chem.* **1981**, *34*, 2035.
(35) Riou, D.; Férey, G. *Eur. J. Solid State Inorg. Chem.* **1994**, *31*, 25.
(36) Soghomonian, V.; Haushalter, R. C.; Chen, Q.; Zubieta, J. *Inorg. Chem.* **1994**, *33*, 1700.

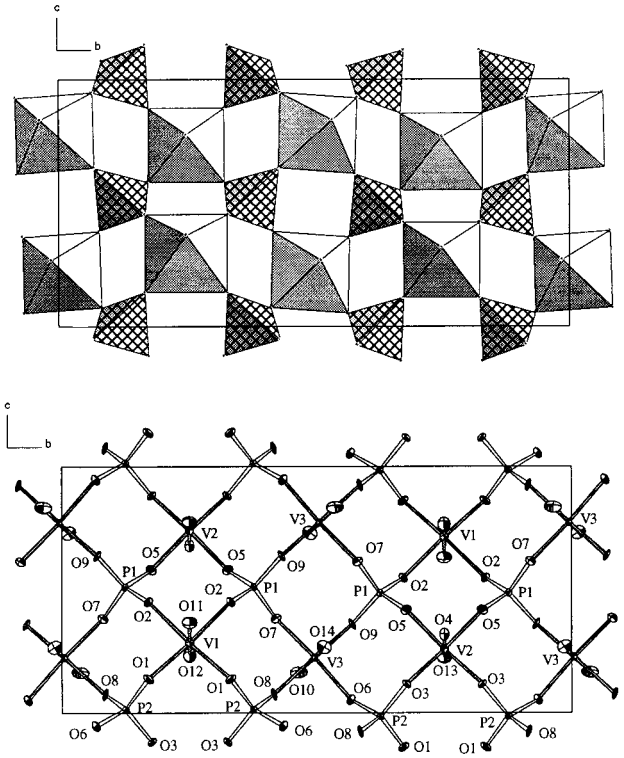

Figure 5. Projection of $VOPO_4 \cdot H_2O$ layers in **2** viewed down the *a* axis. The VO_6 and PO_4 units are shown as empty octahedra and hatched tetrahedra.

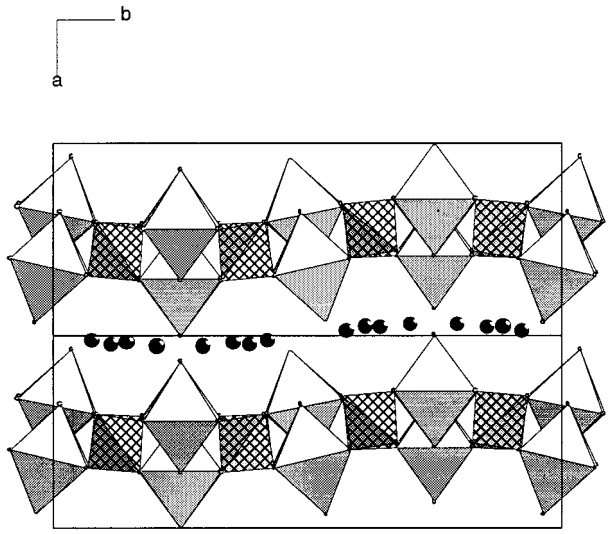

Figure 6. Projection of the structure of **2** in the [001] direction.

of the layers are similar with 6.316 Å (*a*), 6.280 Å $[(b/4)^2 + (c/2)^2]^{1/2}$, and 6.215 Å (*a*) for **1**, **2**, and $VOPO_4 \cdot 2H_2O$, respectively.

In **3**, the $[VO(H_2O)_3]_2[VO(H_2O)][VO(PO_4)_2]_2^{2-}$ framework is built up from six crystallographically distinct VO_6 distorted octahedra and PO_4 tetrahedra. The $V(1)O_6$ octahedra contain one short V=O bond, one long V−OH_2 bond trans to the V=O bond, and four equatorial V−O bonds intermediate in length. The equatorial oxygen atoms are shared with phosphate groups. The $V(2)O_6$ and $V(3)O_6$ octahedra also contain one short V=O bond and one long trans V−OH_2 bond but differ from $V(1)O_6$ in that the coordination in the equatorial plain is completed by two oxygen atoms from phosphate groups and two additional

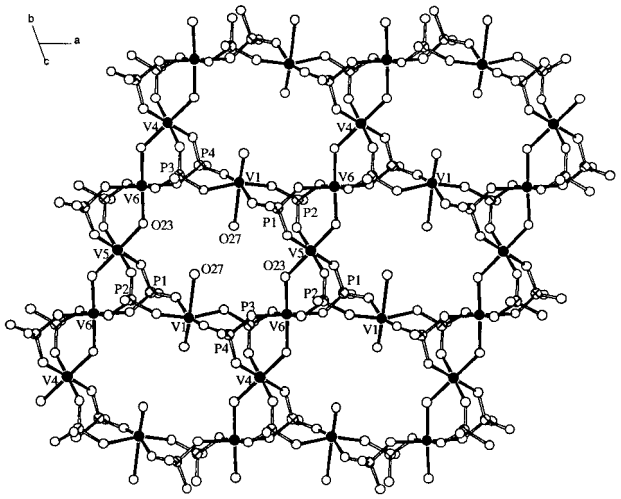

Figure 7. The structure of **3** in the [011] direction, showing the 10-member rings. The vanadium, phosphorus, and oxygen atoms are shown as filled, hatched, and empty circles. V(2) and V(3) atoms are omitted for clarity.

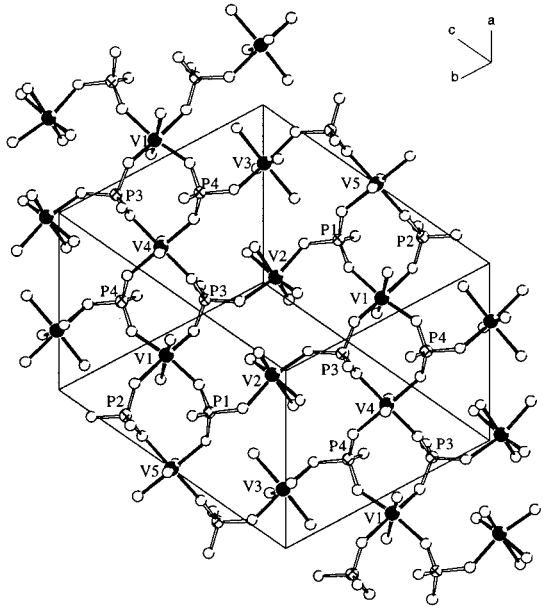

Figure 8. The structure of **3** perpendicular to the (110) planes. The vanadium, phosphorus, and oxygen atoms are shown as filled, hatched, and empty circles. V(6) atoms are omitted for clarity.

water molecules. The BVSs are 4.19, 4.01, and 4.10 for V(1), V(2), and V(3), respectively, in agreement with an oxidation state of V(IV).

The remaining distorted VO_6 octahedra (V(4), V(5), and V(6)) share trans vertexes to form the −V=O−V=O− backbone of an infinite chain in the sequence V(4)−V(6)−V(5)−V(6)−V(4) (Figure 7). The vanadium atom positions are disordered about the center of each octahedron most likely reflecting random −V=O−V=O− orientations of different chains. BVS calculations give values of 3.94, 4.07, and 3.98 for V(4), V(5), and V(6), respectively. Adjacent VO_6 octahedra are bridged by two phosphate tetrahedra, sharing two corners of each tetrahedron to give an overall chain composition of $VO(PO_4)_2$. This chain is closely related to the one found in $(NH_4)_2VO(HPO_4)_2 \cdot H_2O$ and in a number of other hydrogen phosphate phases.[25] Each chain is connected to an adjacent chain through the $V(1)O_5H_2O$ units to form a layer (Figure 7), and the layers are connected by the $V(2,3)O_3(H_2O)_3$ octahedra (Figure 8) to form a three-

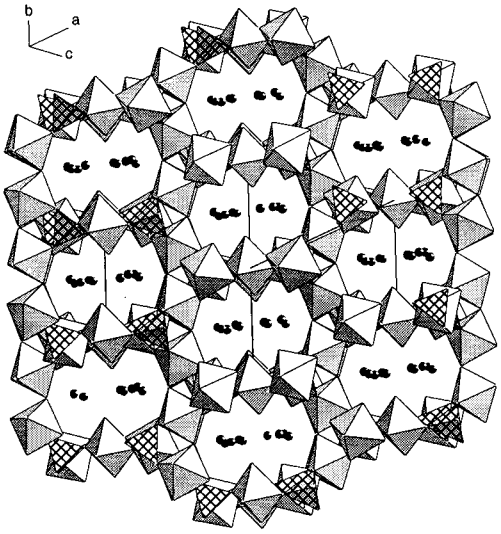

Figure 9. Projection of the structure of **3** in the [111] direction showing the channels. The VO_6 and PO_4 units are shown as shaded octahedra and hatched tetrahedra; NH_4^+ cations and water molecules are shown as filled circles.

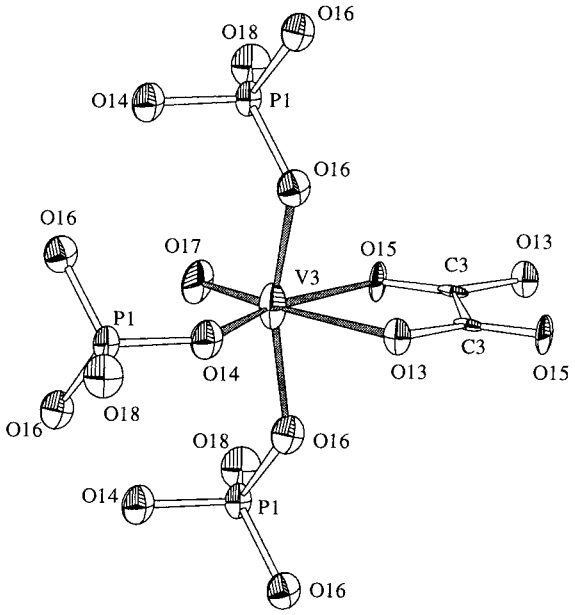

Figure 10. Local geometry of one of the V atoms in **4**. The thermal ellipsoids are shown at 50% probability.

dimensional framework with the composition $[VO(H_2O)_3]_2[VO(H_2O)][VO(PO_4)_2]_2^{2-}$. Two NH_4^+ cations and three water molecules occupy the positions (N1−5) in the channels along the [111] direction (Figure 9).

3 and $(C_4H_{12}N_2)[(VO)_4(H_2O)_4(HPO_4)_2(PO_4)_2]$ have similar framework structures both containing $VO(PO_4)_2$ chains connected to $VO(H_2O)_n$ through the phosphate oxygen atoms.[37] The structures differ in that **3** has no P−OH groups and contains a $VO(H_2O)_n$ octahedron with $n = 1$ in addition to the $n = 3$ type found in both structures.

In the structure of **4,** the V atoms are coordinated by six oxygen atoms to form distorted octahedra. Three of the oxygen atoms are shared as common corners with three PO_3OH groups with typical distances ranging from 1.984(7) to 2.007(5) Å for V(1), 1.973(7) to 2.017(5) Å for V(2), and 1.994(8) to 1.999-

(37) Soghomonian, V.; Haushalter, R. C.; Zubieta, J.; O'Connor, C. J. *Inorg. Chem.* **1996**, *35*, 2826.

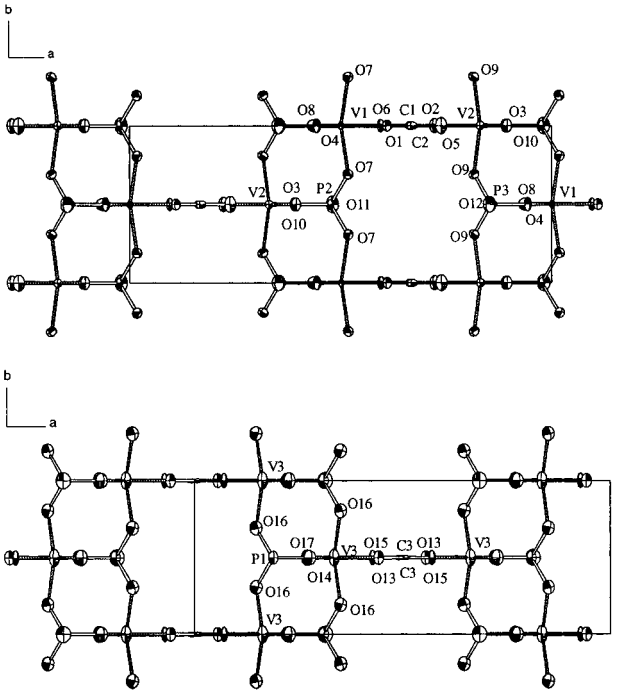

Figure 11. Two crystallographically independent $[VO(HPO_4)]_2(C_2O_4)$ layers in the structure of **4**. The thermal ellipsoids are shown at 50% probability.

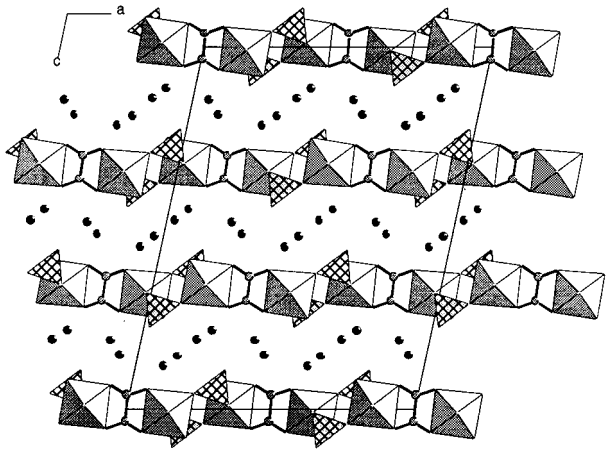

Figure 12. View along the *b*-axis of **4**. Water molecules and ammonium cations occupy the interlayer sites.

(5) Å for V(3). Each of the remaining two oxygen atoms is shared with a C_2O_4 group with longer V−O distances of 2.091-(6) and 2.297(7) Å, 2.074(8) and 2.284(8) Å, and 2.066(7) and 2.321(7) Å for V(1), V(2), and V(3), respectively. The last oxygen atom forms a vanadyl V=O group with a short bond distance (1.609(7) Å, V(1); 1.584(8) Å, V(2); 1.576(8) Å, V(3)). The local coordination of the V atoms is shown in Figure 10. Pairs of vanadium−oxygen octahedra are linked together by a bridging C_2O_4 group in $[V_2C_2O_{12}]$ dimers. Three of the oxygen atoms of the PO_4 groups are shared with the vanadium atoms. The fourth oxygen atom is terminal with long P−O distances of 1.594(7), 1.578(8), and 1.597(9) Å for V(1), V(2), and V(3), respectively, indicating P−OH groups. The bonding between the $[V_2C_2O_{12}]$ dimers and PO_4 groups results in the layers with composition $[VO(HPO_4)_2]_2(C_2O_4)^{2-}$ shown in Figure 11. Four VO_6, two PO_4, and two oxalate units form eight-member rings defined by the positions of O(7)−O(9) (5.208 Å) and C(2)/(1)−C(2)/(1) (6.418 Å) and by O(16)−O(16) (5.195 Å) and

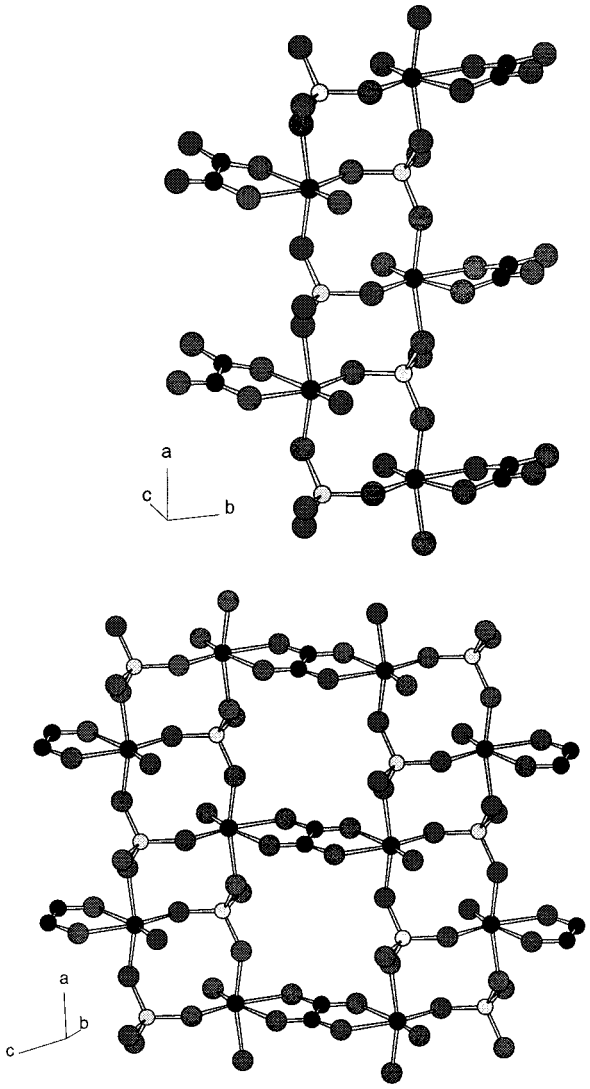

Figure 13. Comparison of the chain and layer structures of $(C_4H_{12}N_2)[VO(C_2O_4)HPO_4]$[10] and $(NH_4)_2[VO(HPO_4)]_2(C_2O_4)\cdot 5H_2O$.

C(3)−C(3) (6.418 Å) (Figure 12). The BVS values calculated for V(1), V(2), and V(3) are 3.97, 4.10, and 4.14, respectively, in agreement with the expected value of 4.00 for V(IV). There are two crystallographically unique $[VO(HPO_4)]_2(C_2O_4)$ layers in the structure. The NH_4^+/H_2O species are located in the space between the $[(VO(HPO_4))_2(C_2O_4)]^{2-}$ layers (Figure 12). An extended network of hydrogen bonds between the oxygen atoms completes the structure in three dimensions.

The layer structure of **4** is related to that of the chain structure of $(C_4H_{12}N_2)[VO(HPO_4)(C_2O_4)]$ as shown in Figure 13. Both structures contain double $[VO(HPO_4)]_2$ chains in which the terminal P−OH groups point in opposite directions alternating up and down along the direction of the chain (Figure 13). Tsai et al.[23] noted the structural relationship between the vanadium phosphate chains in the oxalate compound and a similar double $VO(HPO_4)$ chain found in the $VO(HPO_4)\cdot 4H_2O$[24] structure. In the latter, two water molecules occupy the coordination positions of the oxalate anion. The structural analogy can be further extended by noting the relationship between $(NH_4)_2[VO(HPO_4)]_2(C_2O_4)\cdot 5H_2O$ and $VO(HPO_4)\cdot {}^1/_2H_2O$[38] and $VOSeO_3\cdot H_2O$.[39]

The structure of **4** is related also to the structures of some other metal oxalato−phosphates.[15−22] For example, in the structure of $[C_4H_{12}N_2][In_2(C_2O_4)(HPO_4)_3]\cdot H_2O$,[16] similar $[In_2(C_2O_4)(HPO_4)_2]$ layers are connected together by bridging HPO_4 groups as observed in $N_2C_2H_{10}(VO)_2(PO_4)_2H_2PO_4$ and other related compounds.[40] In contrast, although $[C_2H_{10}N_2]_{2.5}[Al_4H(HPO_4)_4(H_2PO_4)(C_2O_4)_4]$[17] contains bridging phosphate groups, the structure is more closely related to that of $(C_4H_{12}N_2)[VO(HPO_4)(C_2O_4)]$.

Acknowledgment. This work was supported by the National Science Foundation under Grant DMR-9805881 and by the Robert A. Welch Foundation. The work made use of MRSEC/TCSUH Shared Experimental Facilities supported by the National Science Foundation under Award No. DMR-9632667 and the Texas Center for Superconductivity at the University of Houston.

Supporting Information Available: X-ray crystallographic data in CIF format for the structure determinations of **1**−**4**. This material is available free of charge via the Internet at http://pubs.acs.org.

IC0000303

(38) Johnson, J. W.; Johnston, D. C.; Jacobson, A. J.; Brody, J. R. *J. Am. Chem. Soc.* **1984**, *106*, 8123.
(39) Huan, G.; Johnson, J. W.; Jacobson, A. J.; Merola, J. S. *Chem. Mater.* **1991**, *3*, 539−541.
(40) Harrison, W. T. A.; Hsu, K.; Jacobson, A. J. *Chem. Mater.* **1995**, *7*, 2004−2006.